INTERNSHIP REPORT

STUDY OF PASSIVE DAMPING TECHNIQUES TO IMPROVE THE PERFORMANCE OF A SEISMIC ISOLATION SYSTEM

for

Advanced **L**aser **I**nterferometer **G**ravitational Wave **O**bservatory

MASSACHUSETTS INSTITUTE OF TECHNOLOGY

September 2010

Author…….Sebastien Biscans
ENSIM

Advanced LIGO Supervisor……...……Fabrice Matichard
Advanced LIGO Engineer

ENSIM Supervisor……..Charles Pezerat
ENSIM Professor

ACKNOWLEDGMENTS

Many thanks must go out to Fabrice Matichard, my supervisor, co-worker and friend, for his knowledge and his kindness.

I also would like to thank all the members of the Advanced LIGO group with whom I've had the privilege to work, learn and laugh during the last six months.

TABLE OF CONTENTS

1. Introduction

The idea of detecting gravity waves using a laser interferometer was first suggested by Gertsenshtein and Pustovoit (1962). R.Forward built the world's first prototype gravity wave interferometer in the 1970's at Hughes Research Laboratories. This early work was followed by efforts at Munich, Glasgow, MIT, Caltech, Orsay, and more recently ISAS in Japan.

The Laser Interferometer Gravtational Wave Observatory (LIGO) project, cofounded in 1992 by Kip Thorne and Ronald Drever of Caltech and Rainer Weiss of MIT, will use interferometry to directly observe the minute strains in space caused by gravitational wave passing through the Earth. The detector, which is currently under construction in Hanford (Washington) and Livingston (Louisiana), will directly verify the existence of gravitational waves as predicted by Einstein's theory of General Relativity. After establishing the existence of gravitational waves, LIGO will act as an observatory and open the door to gravitational wave astronomy.

LIGO will detect gravitational waves by observing extremely small relative movements in the mirrors at the ends of the interferometer arms. Analytical estimates predict gravitational waves strains in space of 10^{-22} meters (only a fraction of an nuclear diameter over the length of the arm) with event rates of a few per year. The sensitivity of the interferometer is limited by the dominant noise sources shown in Figure 1.

The goal of this internship is to find a groundbreaking solution to reduce the seismic noise (red curve in Figure 1) present in the mirrors, in addition to the work already done those last 18 years.

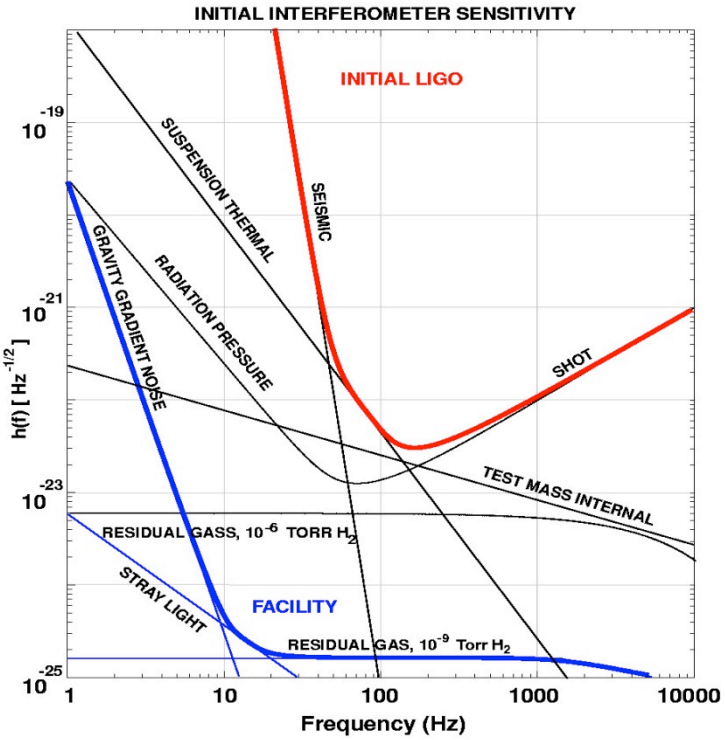

Figure 1 : **Noise specifications for the LIGO sites**

2. Presentation of the seismic isolation system

2.1 General Overview

Sum-total, LIGO is composed of four test masses and a beam splitter, as shown in Figure 2. Actually, a test mass or a beam splitter is an association of two mirrors in series, as shown in Figure 3. Each couple of mirrors is suspended in a pendulum configuration, inside a vacuum chamber. All the system is put in a vacuum environment to limit the local fluctuations. The five chambers are linked together by tubes, a shown on Figure 4.

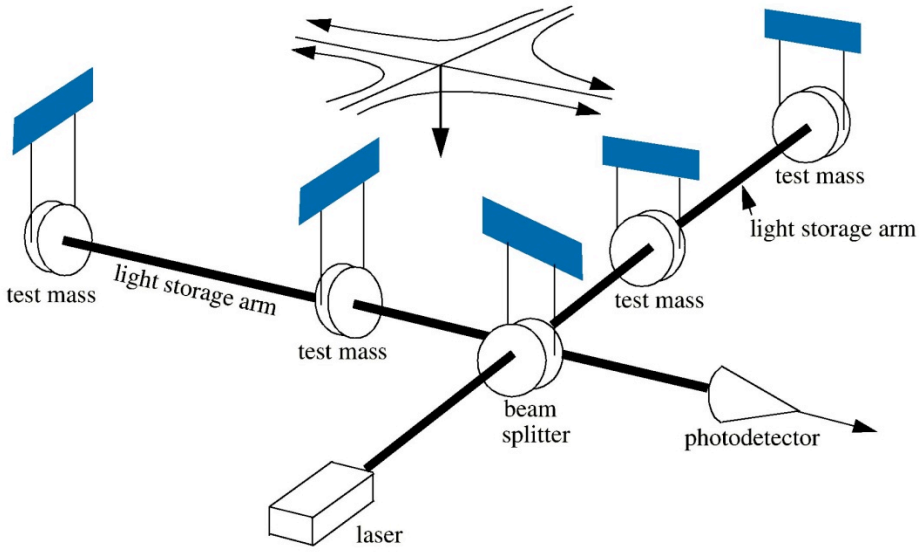

Figure 2 : Working principle of the LIGO Interferometer

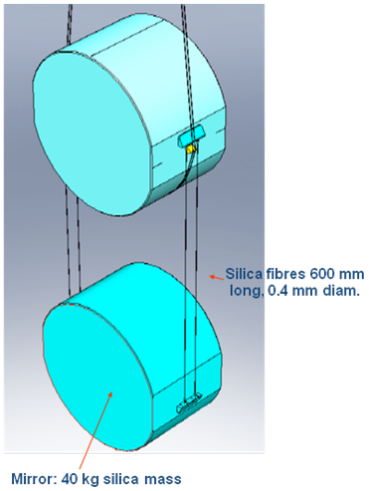

Figure 3 : Illustration of a test mass/beam splitter

a) b)

Figure 4 : a) Model of a vacuum chamber
b) Link tube between the chambers

To control the seismic noise, the pendulum mirrors must be decoupled with the floor. They are attached in a structure called the Quad, which is fixed to the Internal Seismic Isolation system (called BSC-ISI), on the top of the vacuum chamber. Thus, the complete chamber is composed by two mirrors, a Quad structure and the BSC-ISI, as shown in Figure 5.

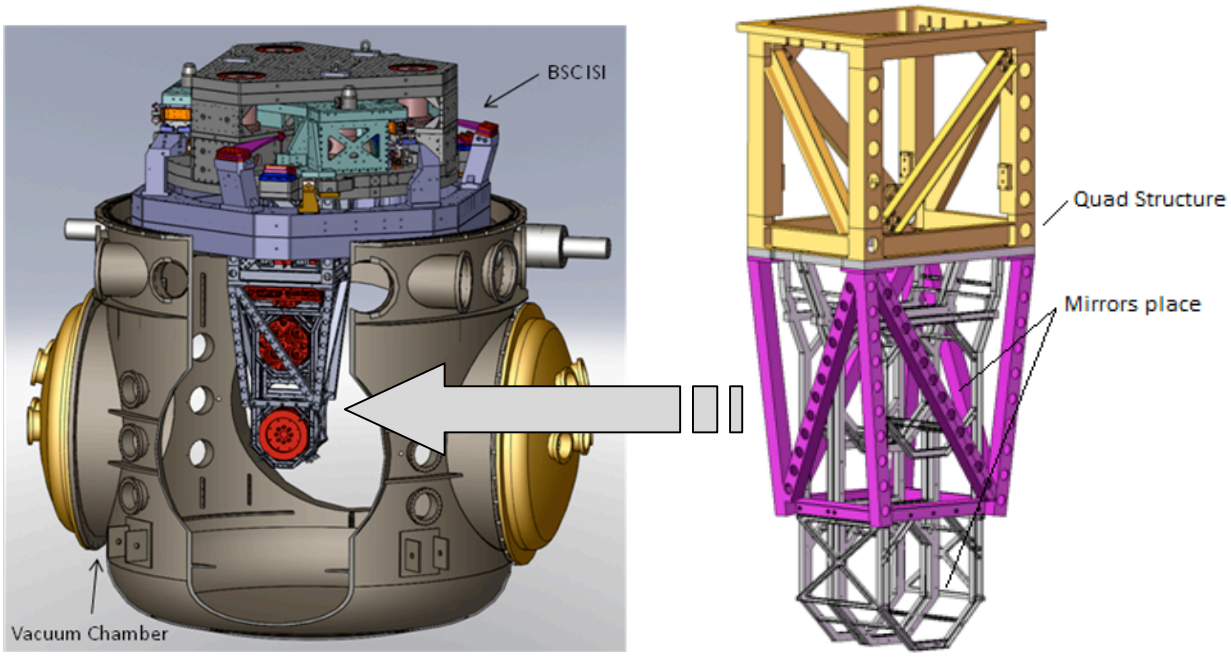

Figure 5 : The complete vacuum chamber

2.2 The BSC-ISI

Each BSC-ISI system is composed of three stages, independent one of the others. Stage 0, the base, is represented in violet in Figure 6. It holds Stage 1, represented in cyan, via blades and flexure rods represented in yellow. The blades provide the vertical flexibility; the rods provide the horizontal one. Stage 1 holds Stage 2, represented in grey, via the same type of blades and flexure rods. The suspended stages have natural frequencies in the 1Hz-7Hz range. The system provides passive isolation above its natural frequencies and active control in the 0.1Hz-100Hz range.

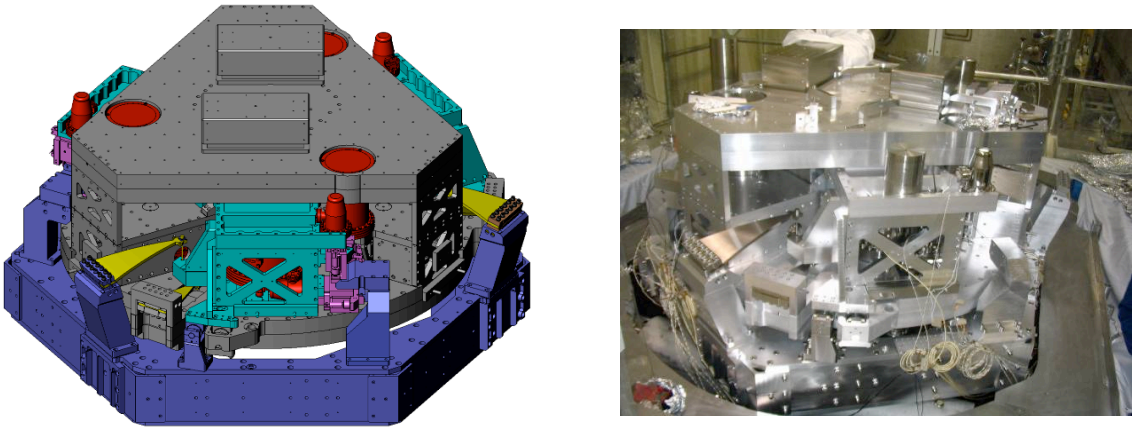

Figure 6 : Presentation of the BSC-ISI system

2.3 The Quad

Each Quad is composed of three parts. The Upper Structure, represents in yellow on the figure 7, and the Lower Structure, in purple, form the external structure. The third part, in grey, called the Internal Structure, is a support for the two mirrors. All this parts are screwed together. Thus the Quad is suspended below the BSC-ISI via the Upper Structure. It presents natural frequencies in the 80Hz-250Hz range.

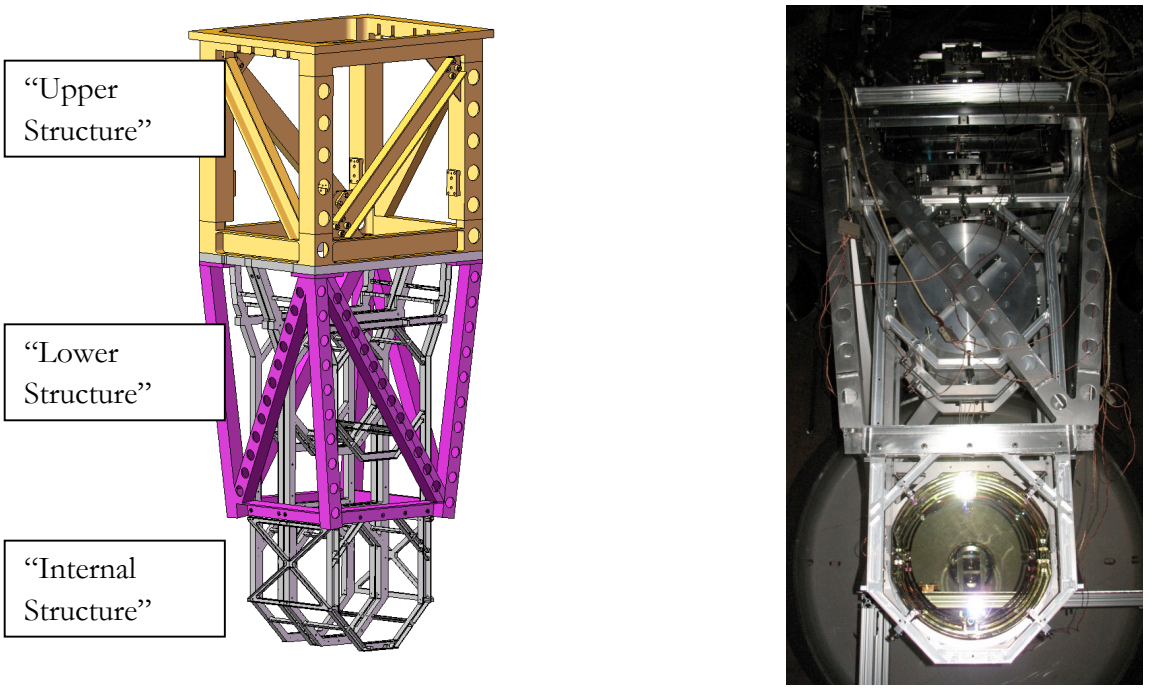

Figure 7 : Presentation of the Quad

The BSC-ISI prototype commissioning allowed us to identify couplings between the platform and the Quad structure suspended from the optical table (Figure 8).

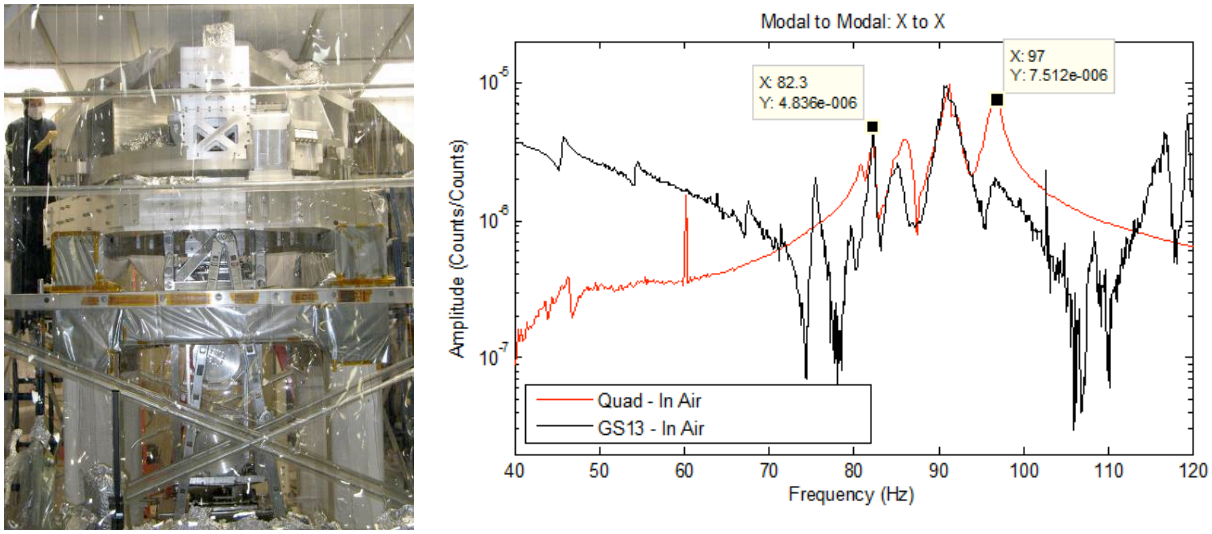

Figure 8 : BSC-ISI transfer function, versus Quad hammering test

This commissioning also allowed to show how important it is to damp some of the structure resonances to improve the global transfer function of the platform. The high numbers of modes and their high Qs are limiting factors of performances and it is a source of instabilities for the seismic platform. Thus, solving these issues with an active method is going to be difficult and not robust. In the next section we present the techniques investigated to damp these resonances.

3. Preliminary study : the tuned mass damper

3.1 Theory

The idea is to damp the natural frequencies of the BSC-ISI and the Quad. That's why we built a tuned mass spring model with four pads of a polymer material (with elastic properties) and a stainless steel mass. Thus, a tuned mass damper is a device that is attached to a structure in order to reduce the dynamic response of the structure. The frequency of the damper is tuned to a particular structural frequency so that when that frequency is excited, the damper will resonate out of phase with the structural motion. Energy is dissipated by the damper inertia force acting on the structure.

This configuration can be represented by a single degree-of-freedom system with structural damping.

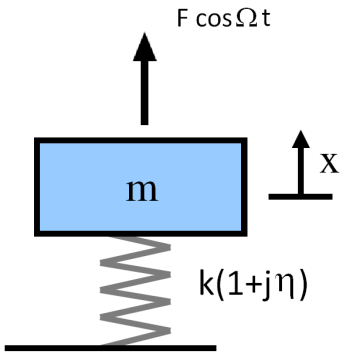

Figure 9 : Single degree-of-freedom system with structural damping

Structural damping is a material characteristic whose value is dependent on temperature and forcing frequency. We consider the excitation as harmonic excitation in the form

$$\vec{F} = F\cos\Omega t = Fe^{j\Omega t} \quad \textbf{(1)}$$

So we have the classic equation of movement

$$m\ddot{x} + c_{eq}\dot{x} + kx = F\cos\Omega t \quad \textbf{(2)}$$

With $c_{eq} = \frac{Ct}{\pi\Omega}$ the coefficient of equivalent damping viscous damping, as it described in '*Mechanical vibrations for engineers*' by M. Lalanne, P.Berthier and J. Der Hagopian. Ct represents a constant depending on the temperature.

m is the mass and k the stiffness of the system.

In complex notation, this becomes

$$m\ddot{z} + c_{eq}\dot{z} + kz = Fe^{j\Omega t} \quad \textbf{(3)}$$

where x = Re [z], the real part of the complex quantity z.

Solutions are sought in the form

$$z = Ze^{j\Omega t} \tag{4}$$

So we can write

$$-m\Omega^2 Z + k(1 + j\eta)Z = F \tag{5}$$

with $\eta = \frac{Ct}{\pi k}$ the loss factor. Finally, we have

$$Z = \frac{F}{k - m\Omega^2 + \mathrm{j}\eta\mathrm{k}} \tag{6}$$

The real part of this expression allows us to see the evolution of the mass displacement x with the frequency.

Firstly, this equation is verified with a loss factor and a stiffness constants, for a resonance frequency equal to f_0 = 100 Hertz, at a temperature of 75°F (23,9 °C).

Parameters :

- Mass : m = 10 lbs = 4.54 kg
- Force apply on the mass : 1 N
- Angular velocity $\boldsymbol{\Omega = 2\pi f_0}$
- Stiffness of the polymer : $\boldsymbol{\Omega = \sqrt{\frac{k}{m}}}$ -> $\boldsymbol{k = \Omega^2 m}$

Work in a vacuum environment imposes a lot of restrains. Thus, for some cleaning reasons, we must used Viton© as a polymer material. The loss factor η_{100} = 0.7.

All the parameters are injected in the Z expression.

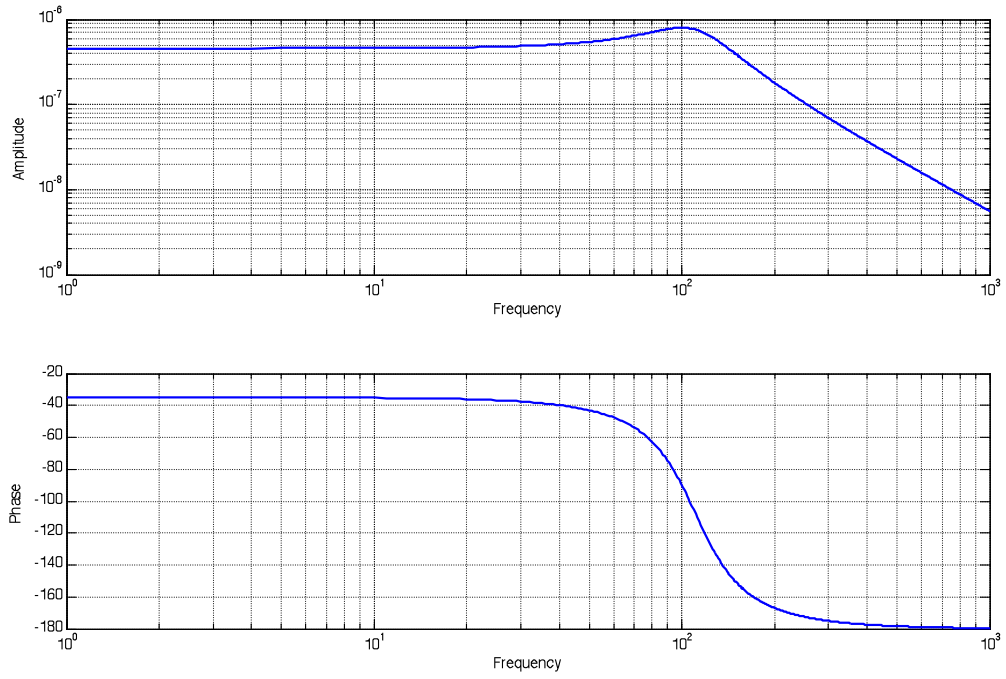

Figure 11 : Representation of the amplitude and the phase of the complex quantity Z when k and η are constants

As we expected, we obtain a typical evolution of the displacement with a pick at the resonance frequency and a damping effect after it.

The interesting part it is now to observe the behavior of the displacement with a changing value of the loss factor and the stiffness. But the Young modulus can be written depending on the stress σ and the strain ε of the polymer material.

$$\sigma = E\varepsilon \tag{7}$$

If we consider the force applied as uniform on all the surface of the mass, the expression becomes

$$\frac{F}{S} = E\frac{\Delta h}{h} = E\,\frac{x}{h}\;; F = E\frac{S}{h}x \text{ , so } k = E\frac{S}{h} \tag{8}$$

with S the total surface and h the thickness of the polymer material.

For the precedent case, we have E_{100} = 2.2*10^3 psi = 15.17*10^6 Pa

$$\frac{S}{h} = \frac{k}{E} \tag{9}$$

If we fix the thickness of the material, we can determine easily the associated surface, and so the size required for the polymer material to have the frequency response chosen.

Finally the stiffness depends on the Young modulus evolution. We have different values of the Young modulus and the loss factor : at 10 Hz, 100 Hz, 1000 Hz, 10000 Hz. The principle seismic

noise which perturbs the BSI-ISI is linked at frequencies between 0 and 1000 Hertz. In a first approach, we do a linear interpolation of the Young modulus value (and so the stiffness value) and the loss factor between 10 and 100 Hertz, and between 100 and 1000 Hertz.

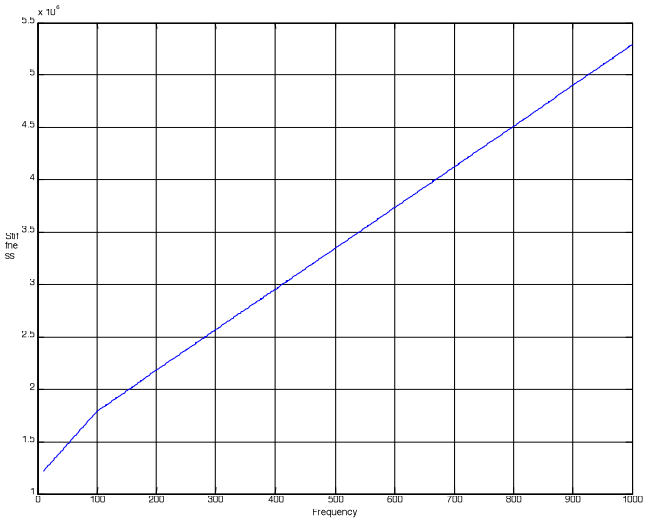

Figure 12 : Evolution of the stiffness with the frequency

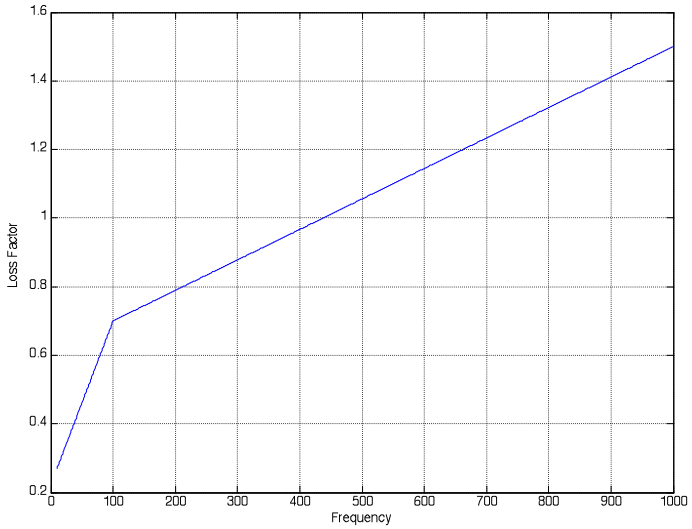

Figure 13 : Evolution of the loss factor with the frequency

This evolution allows us to calculate two affine functions describing the evolution of the stiffness and the evolution of the loss factor with the frequency. These two functions are injected in the Z equation to calculate a new behavior of the system.

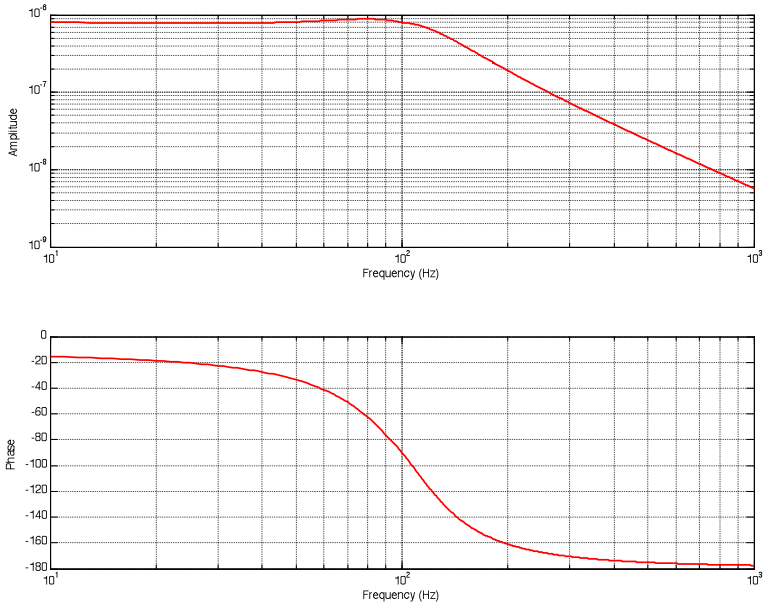

Figure 14 : Representation of the amplitude and the phase of the complex quantity Z when k and η are changing in a linear way

Thi model predicts a really damped displacement at the resonance frequency. This observation shows that it is not necessary to tune very precisely the mass damper. The next step is to check the validity of this solution in practice.

3.2 Experimental verification

3.2.1 Static stiffness

Some samples of the polymer material (Viton© material) are available to test different sizes and forms.

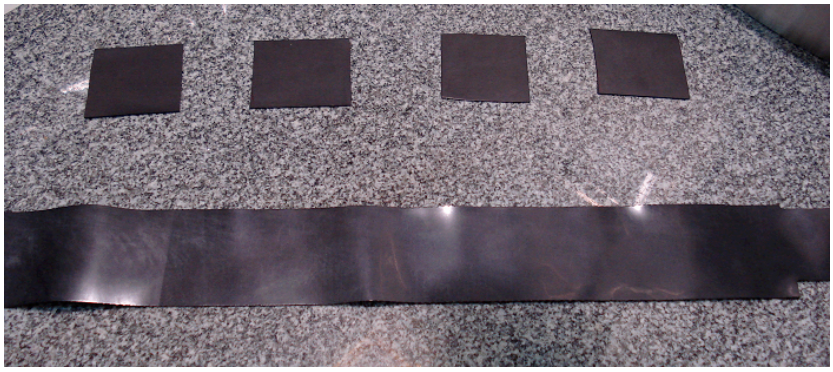

Figure 15 : Samples of Viton©

For a good control of the Viton© characteristics, a static study of the material used is made in a first time. It consists to calculate the Young modulus of the Viton© thanks to evolution of the stress with the strain. The aim is to compare the experimental value with the theoretical value to estimate the error done in our model.

In a first time, it is not possible to do the experience with the real masses of the system, so it is made with masses of 10, 20, 30 and 40 lbs (4.54 kg, 9.07 kg, 13.61 kg and 18.14 kg). Four square pads of Viton© are put under an aluminium plate. The weight of this plate is gradually increased and decreased by a game of masses on it, to 10 lbs to 100 lbs. This addition of weight on the plate leads to a deformation of the Viton©, measured thanks to several dial gauges.

Figure 16 : General scheme of the experience used to determinate the static Young modulus of the Viton©

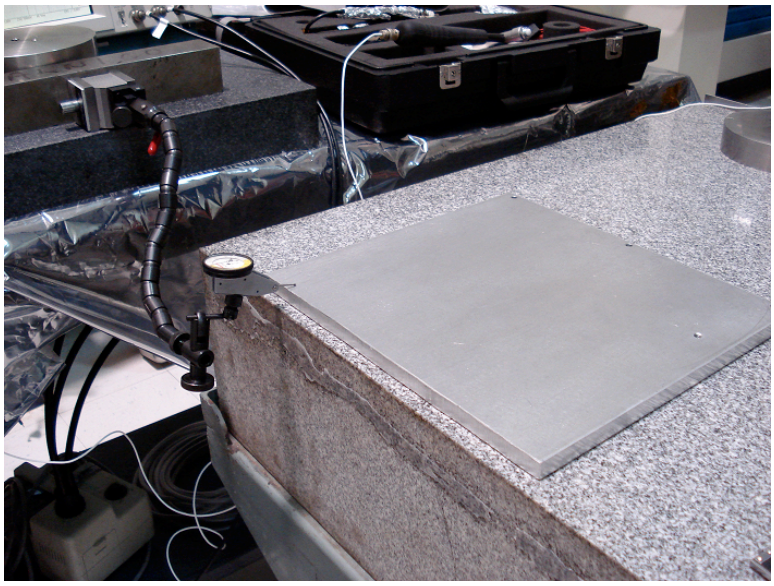

Figure 17 : Photography of the test bench used to characterize the Viton©

Knowing the force F applies by the masses, and the total surface S of the pads, we can calculate the stress applied. Moreover, knowing the thickness h of the material, and the deformation Δh of the Viton© under the stress action, we can find the strain of the material.

Samples characteristics :

- 4 square pads in each corner of the plate
- Thickness -> h = 0.8 mm
- Size of a side of one pad -> b = 6 mm
- Total surface of the pads -> $S = b^2*4 = 144\ mm^2$

The measurement is realized when the plate is loading and unloading, to observe the hysteresis variation of the young modulus.

Two different types of samples are tested. Three series of measures are done for each.

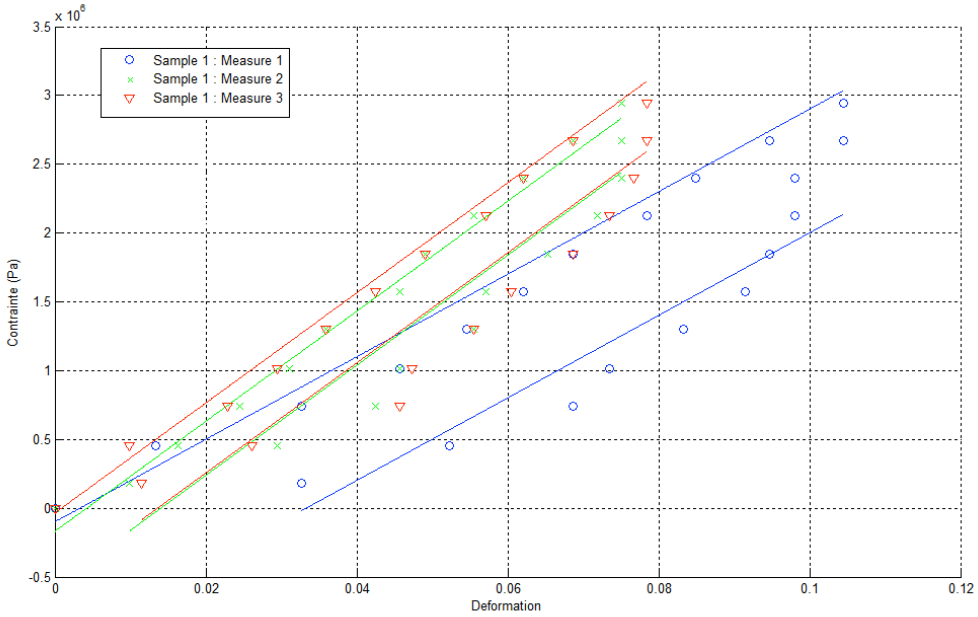

Figure 18 : Evolution of the stress with the stiffness of the Viton© material – Sample 1

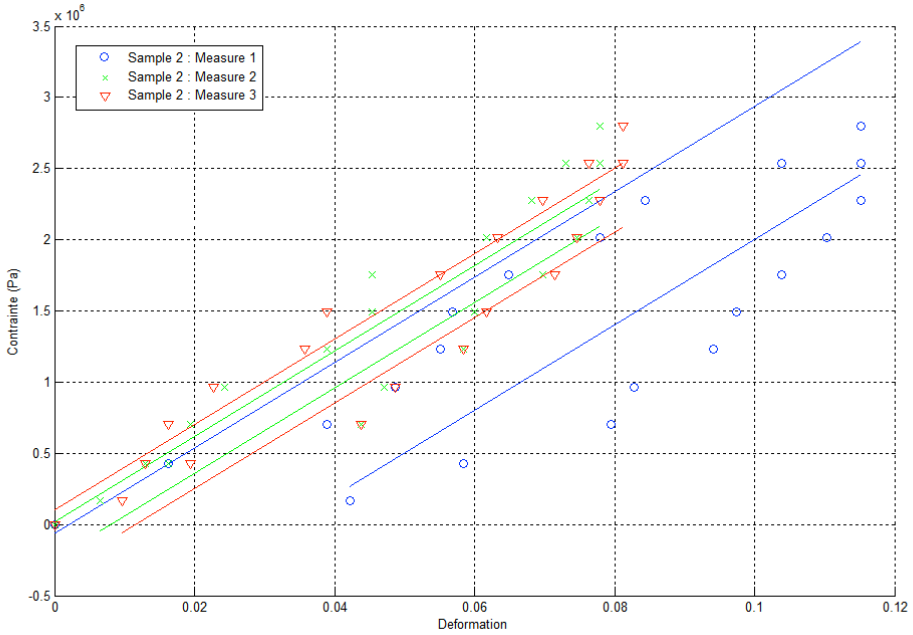

Figure 19 : Evolution of the stress with the stiffness of the Viton© material – Sample 2

The Viton© cut is done manually, that is suppose a sizeable uncertainty on our results. Given that, we could plot two linear regression curves for each series of measure : one for the loading measurement and one for the unloading.

These curves represent on the figures 18 and 19 allow us to calculate directly the Young modulus, which corresponds to the slope of each curve.

	Sample 1			Sample 2		
	Measure 1	Measure 2	Measure3	Measure 1	Measure 2	Measure 3
Load	30 MPa	40 MPa	40 MPa	30 MPa	30 MPa	30 MPa
Unload	30 MPa	40 Mpa	40 MPa	30 MPa	30 MPa	30 MPa

Table 1 : Calculation of the static Young modulus for the different measures

According to the results exposed in table 1, the average Young Modulus of the Viton© is 33 MPa. In the literature, the static Young modulus found is around 15 MPa. So we have a factor of two between theory and practice. This difference can be the result of two facts :

- The experimental set up is not good. This explanation is the most probable, because is very difficult to do a good measure of the plate displacement (very small value).
- The result is good in our conditions.

Anyway, even if the result is false, the goal of this project is to tune the Viton© at the resonance frequency we want. The characterization of the Viton© is not our first aim.

Thus the next step is now to observe the behavior of the material in a dynamic point of view.

3.2.2 Dynamic stiffness

The experience is done on a marble bench, theoretically uncoupled with the floor. The mass is excited by an impact hammer with a force measured. The resultant vibration in the system is collected by in accelerometer fixed on the mass. The hammer and the accelerometer are linked to an oscilloscope to check the quality of obtain signals and to a signal analyzer. This signal analyzer allows us to obtain the frequency response of the system. Thanks to the frequency response, we can calculate the displacement of the mass and see the action of the Viton©, especially the resonance frequency.

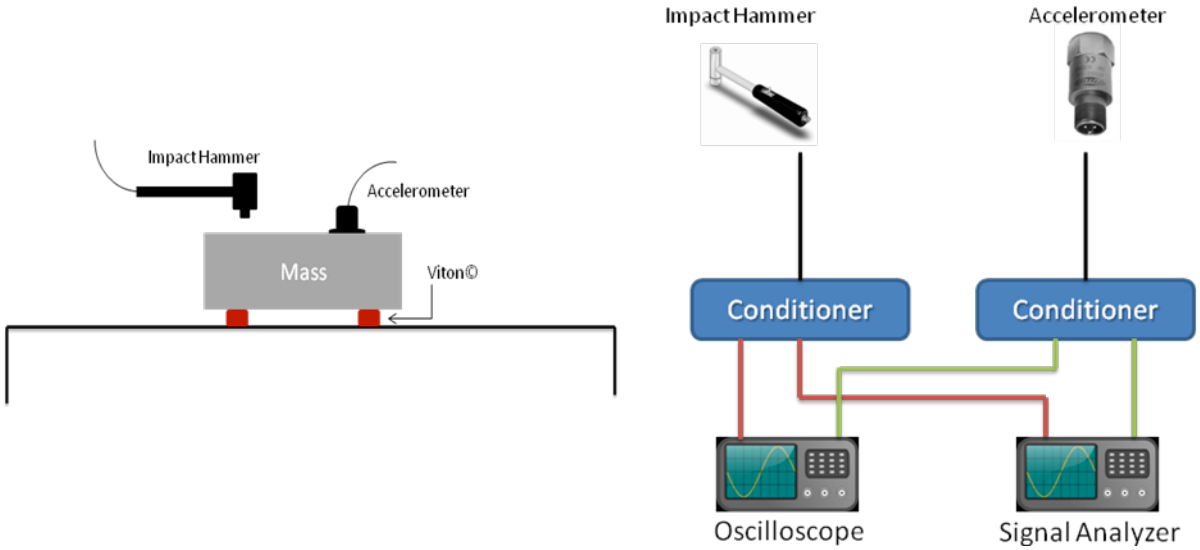

Figure 20 : Description of the dynamic experience used to find the evolution of the resonance frequency with the size of Viton©

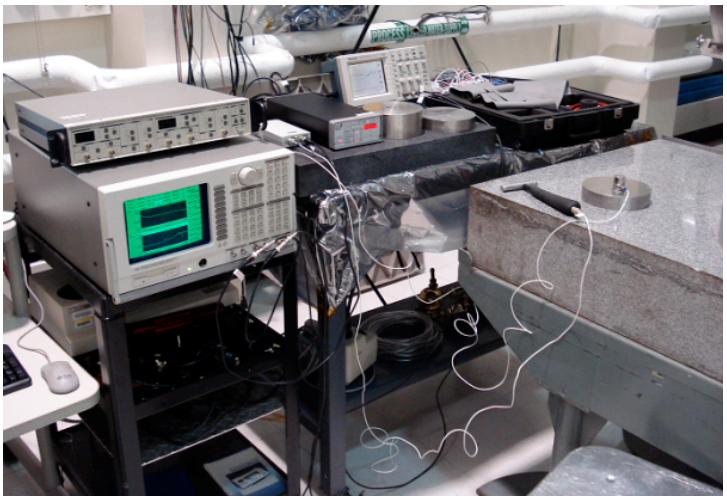

Figure 21 : Photography of the dynamic test bench

According to the theory, if we want a resonance frequency at 100 Hertz, we need a total surface S under the mass equal to :

For a 10 lbs mass :

$$\frac{S}{h} = \frac{k_{100}}{E_{100}} \Longrightarrow s = \frac{hk_{100}}{E_{100}} = \frac{0.067 * (2\pi * 100)^2 * 10}{2.2 * 10^3} = 0.31\ in^2 = 2.00 * 10^{-4}\ m^2 \quad \textbf{(10)}$$

If we use four square pads of Viton©, the size of a side of one pad is :

$$\sqrt{\frac{0.31}{4}} = 0.28\ in = \ 7.1\ mm \qquad \textbf{(11)}$$

For a 20 lbs mass :

$$\frac{S}{h} = \frac{k_{100}}{E_{100}} \implies s = \frac{hk_{100}}{E_{100}} = \frac{0.067 * (2\pi * 100)^2 * 20}{2.2 * 10^3} = 0.62\ in^2 = \ 4.00 * 10^{-4}\ m^2 \qquad \textbf{(12)}$$

If we use four square pads of Viton©, the size of a side of one pad is :

$$\sqrt{\frac{0.62}{4}} = 0.39\ in = 1\ cm \qquad \textbf{(13)}$$

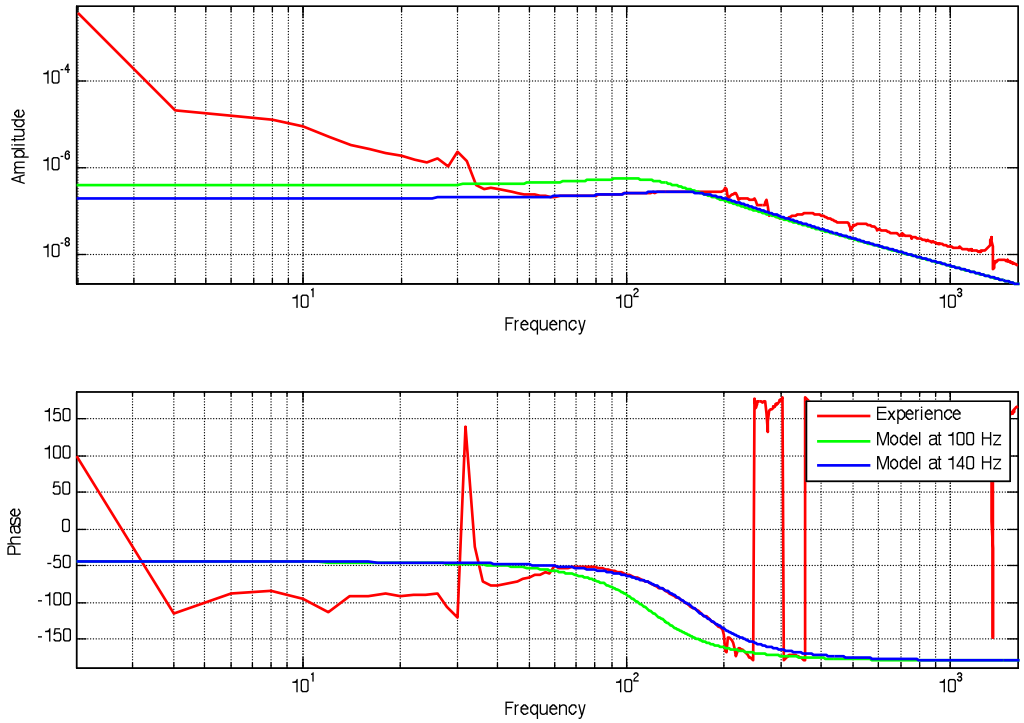

Figure 22 : Characterization of the resonance frequency of a tuned mass damper. The size of the Viton© side is 7.1 mm (m=10 Lbs)

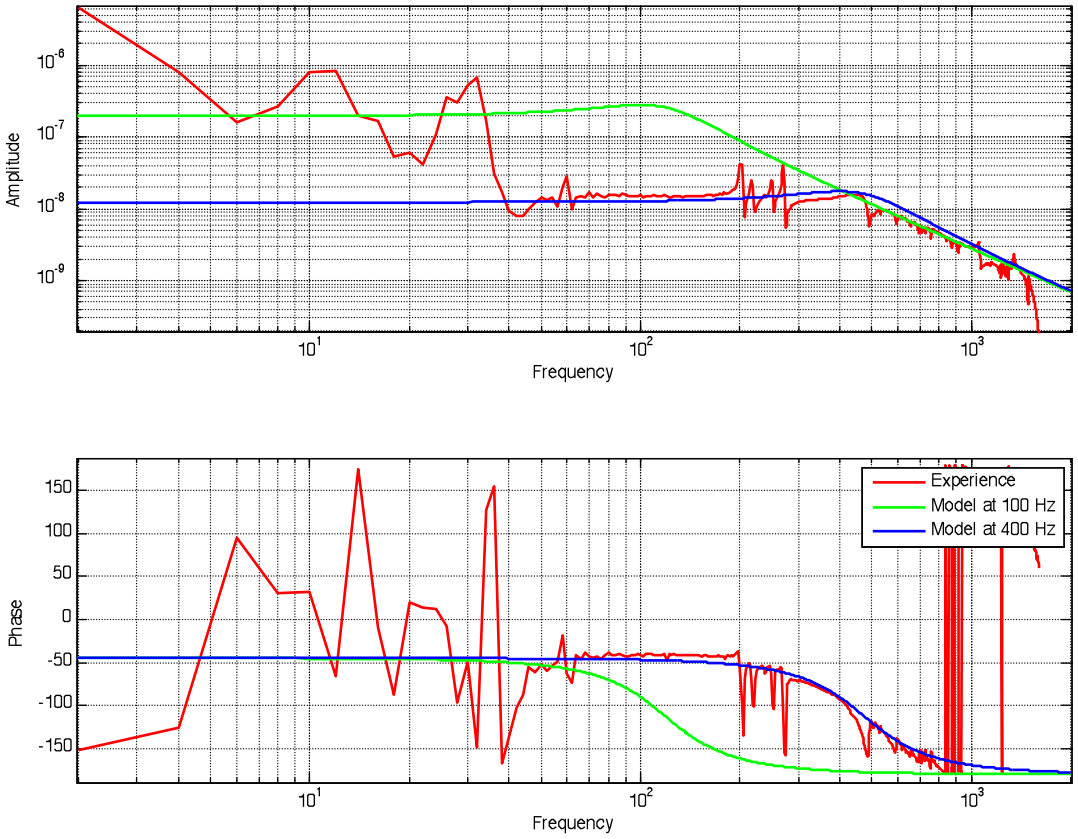

Figure 23 : Characterization of the resonance frequency of a tuned mass damper. The size of the Viton© side is 1 cm (m=20 Lbs)

With the 10 lbs mass, the frequency resonance is 140 Hertz, and it is 400 Hertz with the 20 lbs mass. Thus we obtain two different resonance frequencies, and a big difference between the theory and the practice. After many tests, the conclusion is it is very difficult to well characterize the Viton© behavior. So before to continue, we have to find coherence between our reasoning and the practice.

Logically, if the surface of the pad is reduced by two, the stiffness of the pads is also divided by two, and so the resonance frequency by $\sqrt{2}$.

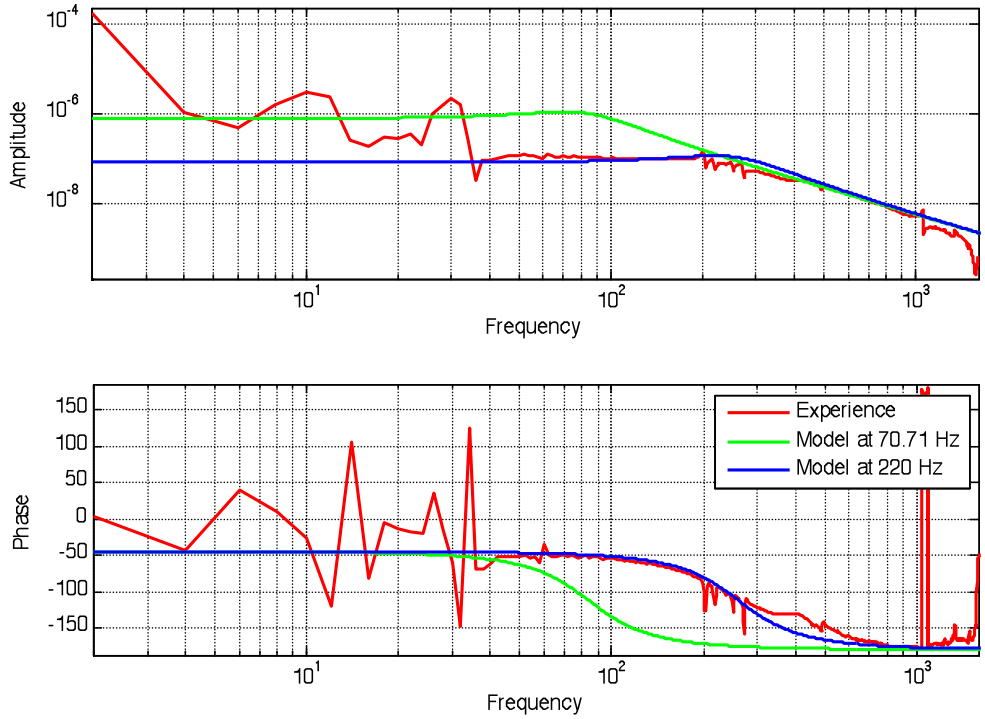

Figure 24 : Characterization of the resonance frequency of a tuned mass damper. The size of the Viton© side is 5.02 mm (m=10 Lbs)

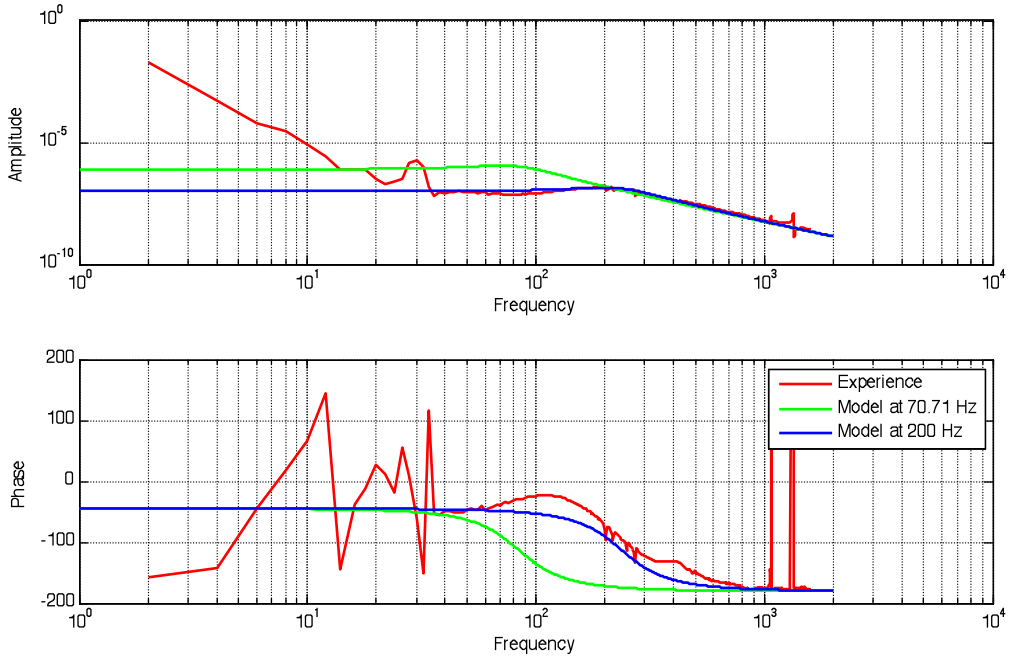

Figure 25 : Characterization of the resonance frequency of a tuned mass damper. The size of the Viton© side is 7.07 mm (m=20 Lbs)

These results prove that the beginning reasoning is false. A finite element analysis has also be done, but the conclusion is the same : the behavior of the Viton© seems non-linear and unpredictable.

Nevertheless, even if we cqn predict the frequency resonance, the mass spring device seems positive and the next step is to investigate on the real system in an empirical way.

4. Design

4.1 Mass Damper on the BSC-ISI

A lot of masses are put on the BSC-ISI to stabilize it. In order to damp Stage 2 vibrations, the idea is to use all these masses to create some tuned mass dampers. Several pads of Viton© are put between the masses and the stages. Almost 200 lbs are used as mass dampers (approximately 20% of the platform)

4.2 Mass Damper on the Quad

To damp the resonance frequencies of the Quad, we used a new system called a vibration absorber. A vibration absorber is a device that is attached to a structure in order to damp the resonances. Vibration energy is dissipated by the vibration absorber.

The difference between a vibration absorber and a classic tuned mass damper system, is that the frequency of the vibration absorber does not need to be tuned : the damping action is broadband and is going to be efficient on all the low frequency modes of the structure. Moreover, this device can be handle easily during the installation.

A mass spring system is made of a 4 lbs stainless steel mass and Viton© pads. It is put in a box, made of two clamps. The system can be attached on several locations on the structure, thanks to two attachment brackets. The stress applied on the pads can be controlled by the use of precision washers.

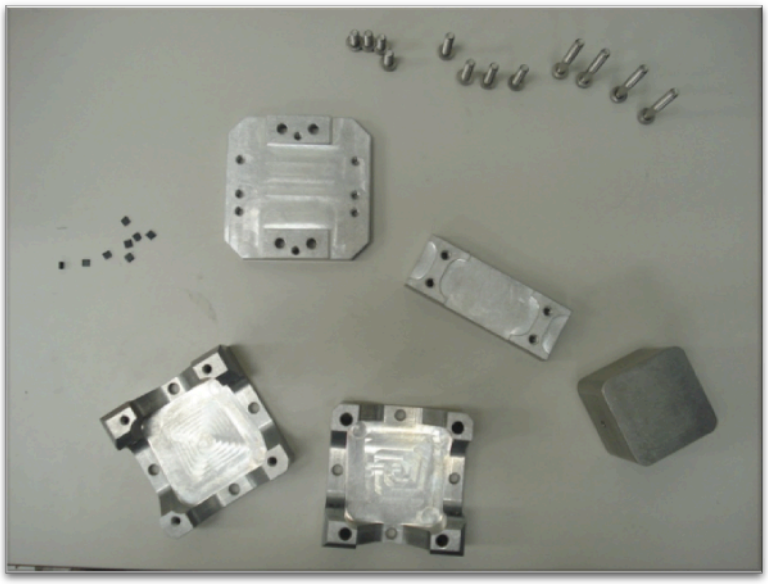

Figure 26 : Parts of a vibration absorber

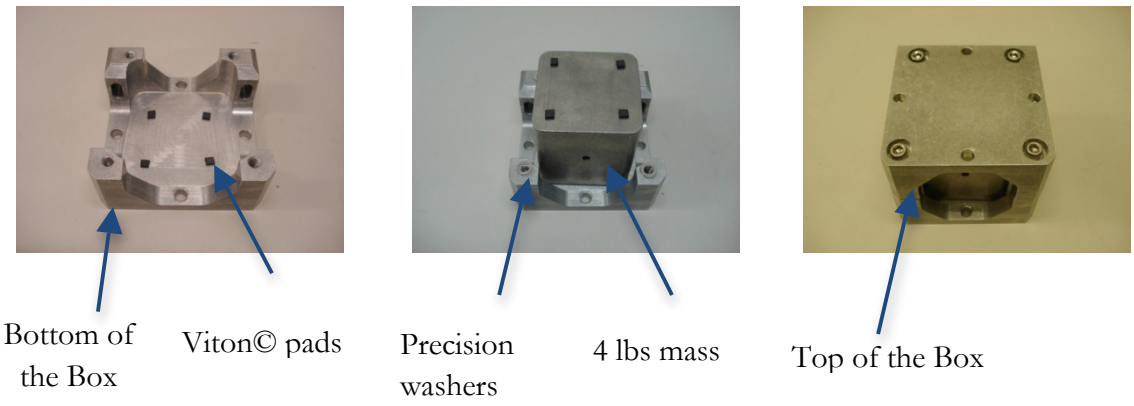

Figure 27 : Assembly steps of a vibration absorber

The absorber can be attached to in two configurations:

- Horizontal layer: the pads are in the horizontal plan. The Viton© works mostly in shear.

- Vertical layer: the pads are in the vertical plan. The Viton© works mostly in compression.

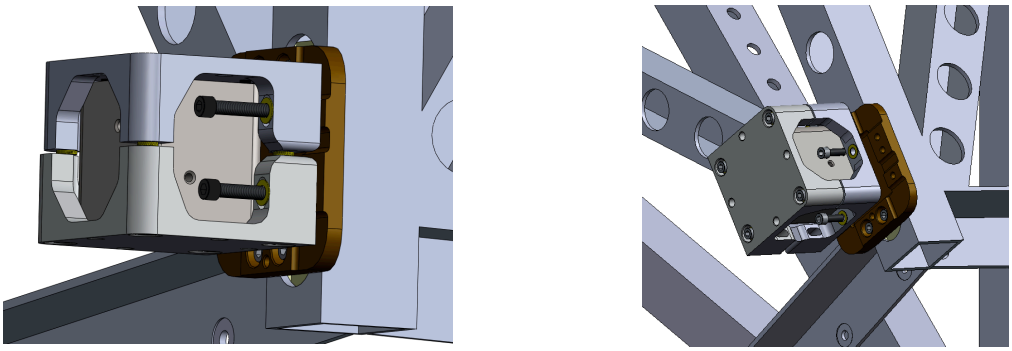

Configuration 1 : Viton© layer in the horizontal plan

Configuration 2 : Viton© layer in the vertical plan

Figure 28

5. Experiment

5.1 BSC –ISI

Both suspended stages (Stage 1 and Stage 2) have six degrees of freedom (three translations, three rotations). Thanks to an association of sensors and actuators, we can measure the transfer function of the two stages in all the directions (Stage 0, grounded to the floor, allows less issues and will not be study during this internship).

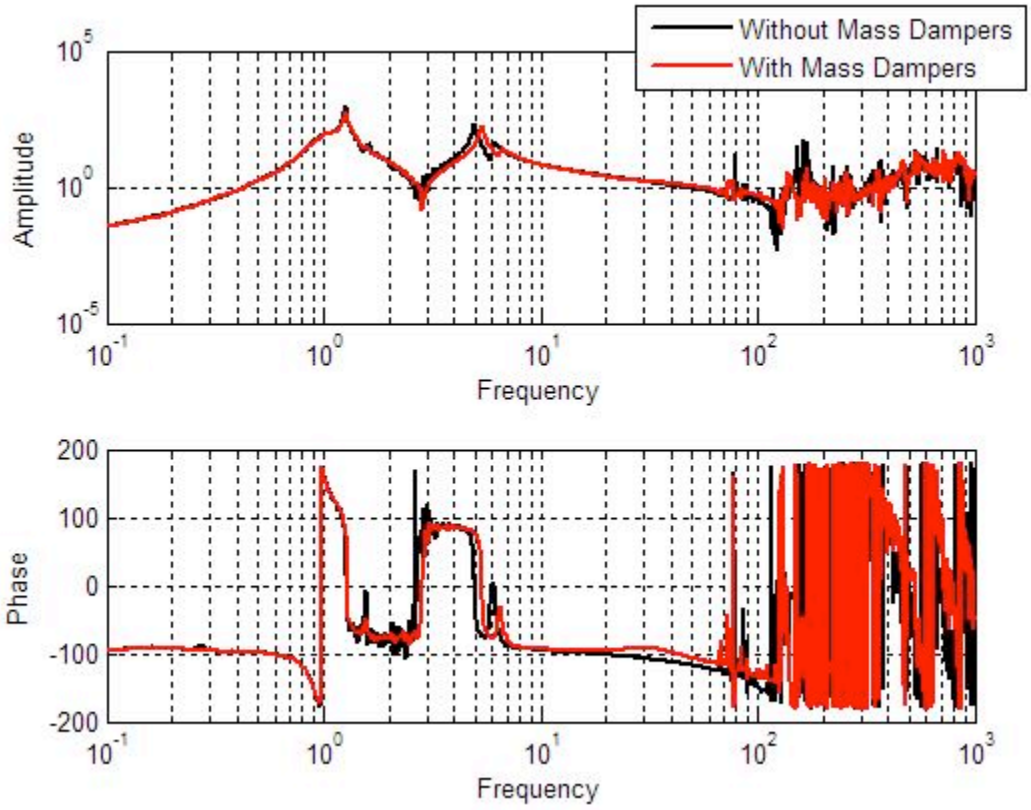

Figure 29 : Transfer functions of Stage 2 in all the six degrees of freedom (in vacuum)

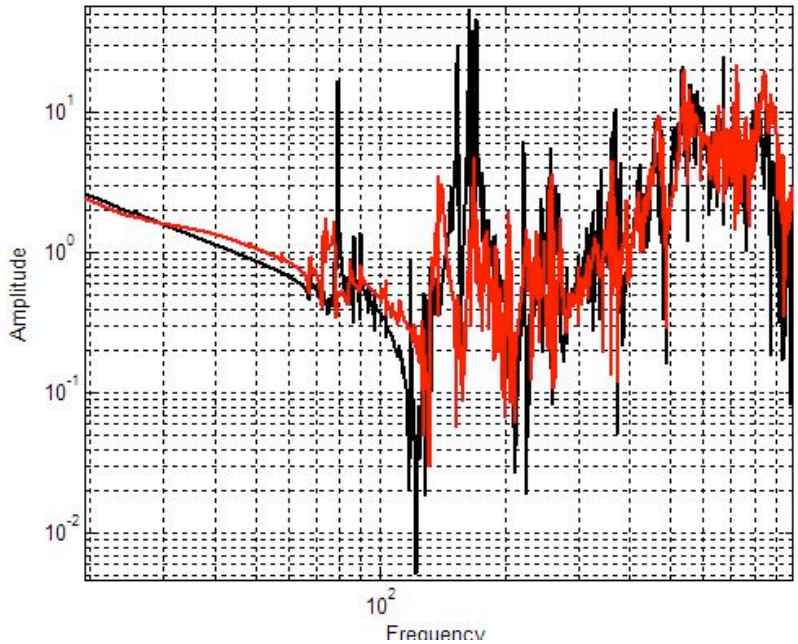

Figure 30 : Transfer functions of Stage 2 - Zoom

Firstly, we can see a lightening effect around 30 Hertz, the frequency resonance of the mass damper: before the frequency resonance, the mass of the mass damper is coupled with the platform. After this frequency, the mass becomes uncoupled and a lightening effect appears.

Given that, we can see a lot of resonances between 70 Hz and 1000 Hz. With the mass damper, the first resonance is very well damped, and in a general view, the curve is smoothed by at least a factor of 3.

5.2 Quad

All the experimentations are done in the air on a Quad prototype. This prototype is only made of the upper structure and the sleeve. We did not have the internal structure.

It would have been more realistic to attach the Quad on an optic table. However, the bench we were using for the preliminary testing was not anymore available. Thus, the Quad is suspended by four hooks to make a free structure analysis. This configuration alters the analysis, but should allow to demonstrate the vibration absorber efficiency.

The modal analysis is done using an accelerometer on the Quad and an impact hammer with force sensor. The accelerometer is clamped on the upper structure. The impact is applied on the upper structure.

Transfer functions of accelerometer response over the impact force are taken. The input/output points are shown on the picture above.

This configuration gives us a characteristic transfer function of the quad. The TF is made of 10 data averaging.

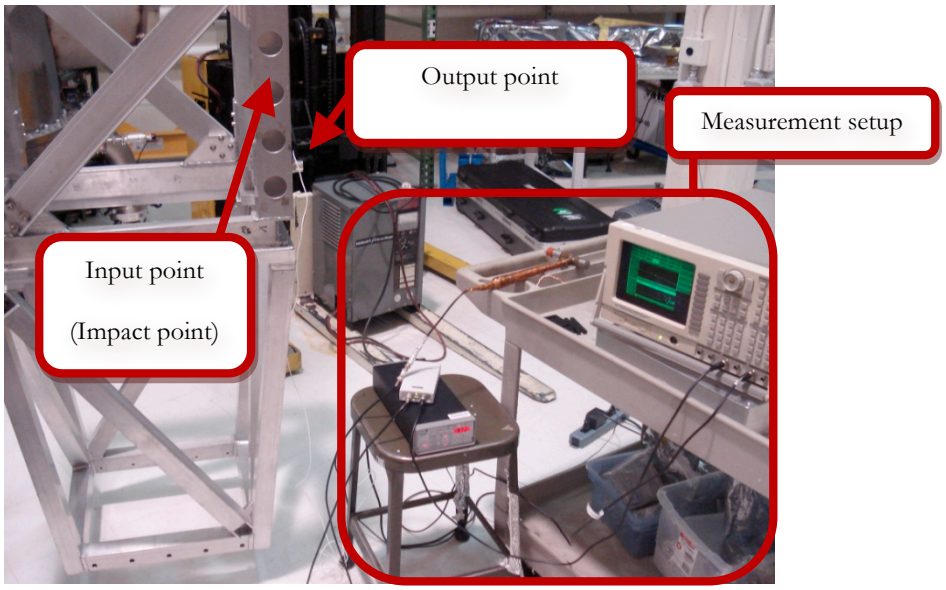

Figure 31

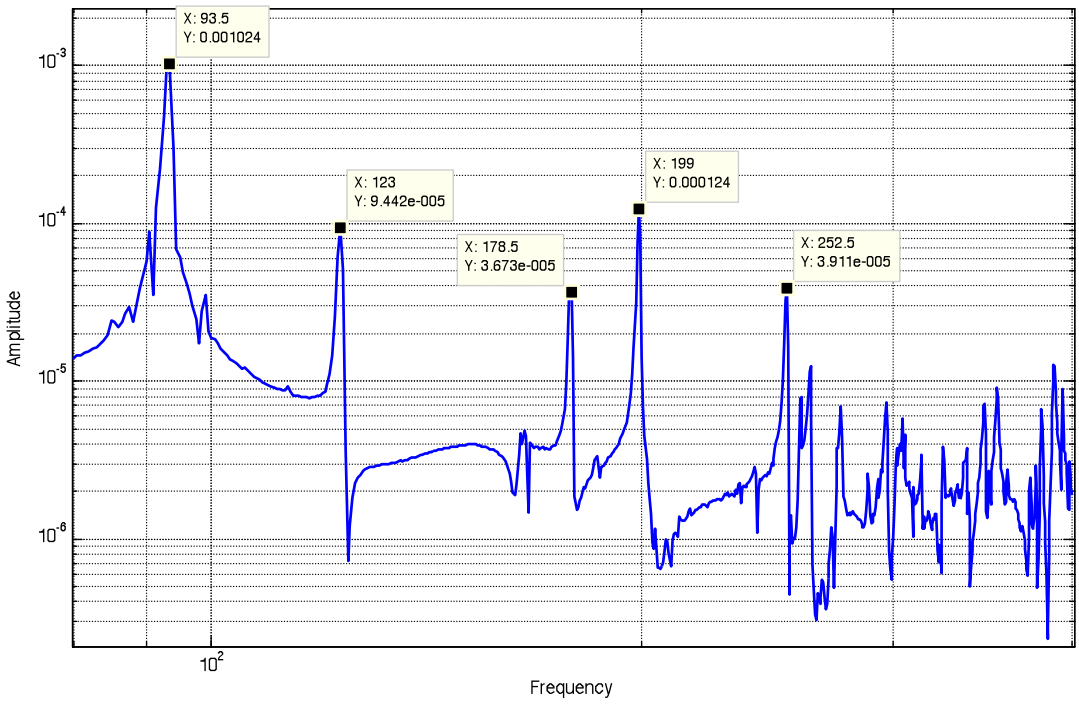

Figure 32

The Quad prototype structure has five main modes between 90 Hz and 260 Hz. These modes are partially damped by the air and are likely to have a higher Q in the vacuum.

The vibration absorber is attached on the Quad thanks to two plates (plate 1 + plate 2). Those two plates are bolted together and then attached on the quad.

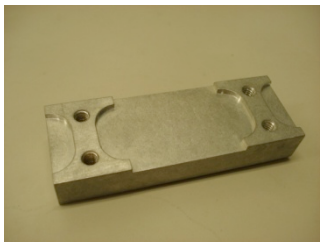

Plate 1

+

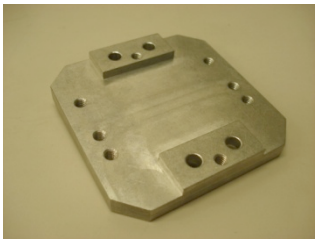

Plate 2

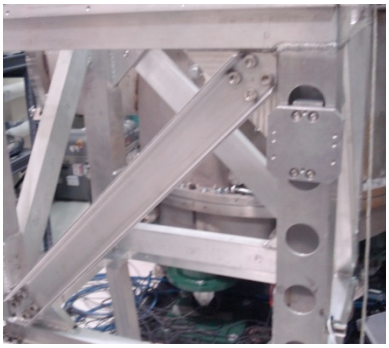

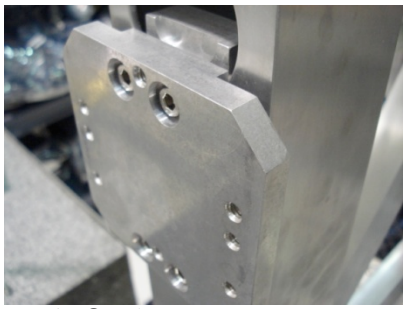

Figure 33 : assembly of the vibration absorber on the Quad

The vibration absorber is attached on plate 2.

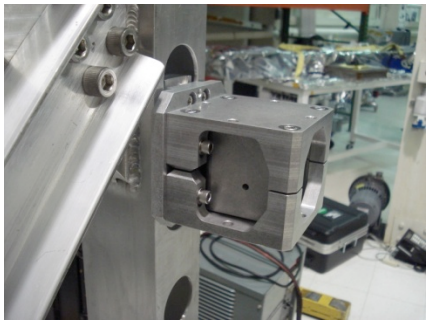

Configuration 1

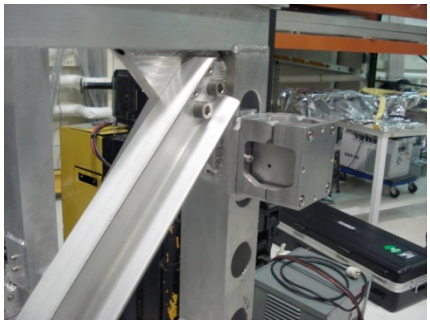

Configuration 2

Figure 34

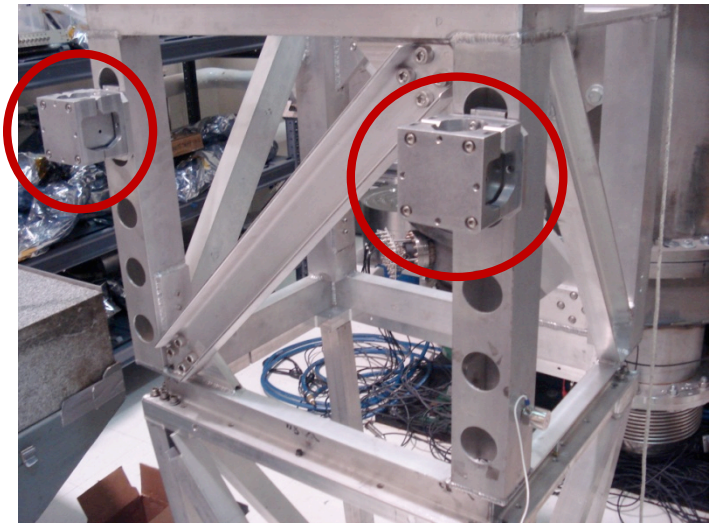

Figure 35 : Vibration absorber on the Quad

After a lot of tests and adjustment, the best configuration is :

- One vibration absorber
- Pads in the horizontal layer
- Soft pads
- The load applies by the top clamp must be as lower as possible

Results are presented below.

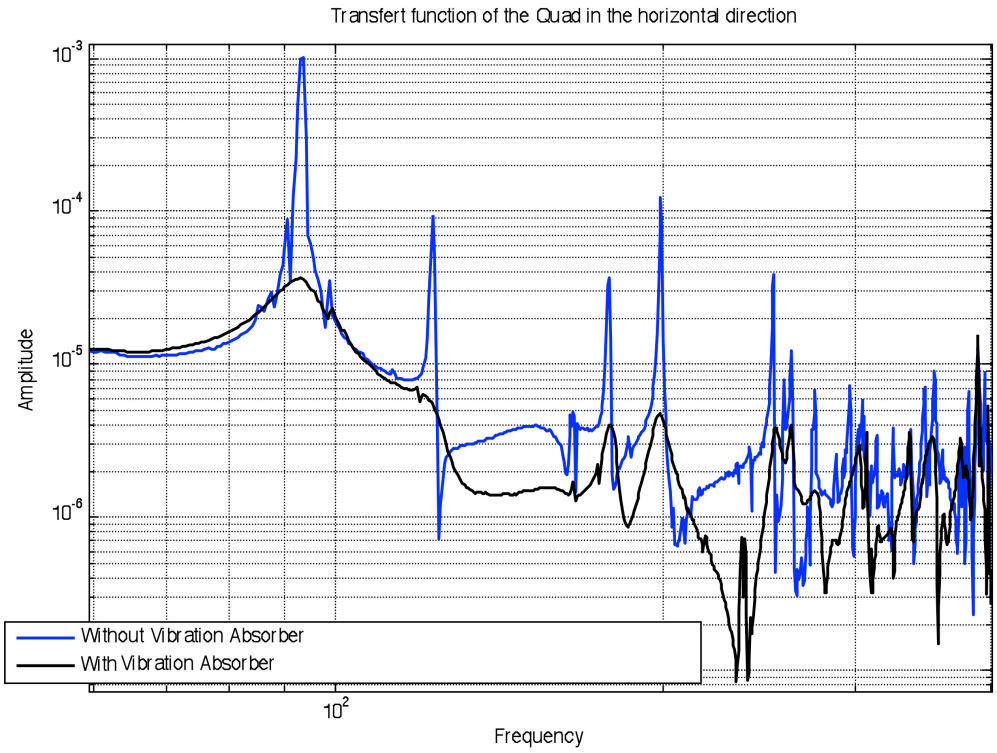

Figure 36 : transfer function of the Quad in the horizontal direction

Without vibration absorber, we can see five modes between 90 Hz and 300 Hz. With one vibration absorber, the first mode is very well damped. Thanks to the vibration absorber, the mode at 93 Hz goes from a factor Q equal at 18 to a factor Q of 2.

To confirm these good results, the next step is to work on the real Quad in a vacuum environment. Unfortunately, this part could not be done before the end of the internship.

Finally, a simple device has been found to damp the majority of modes of the seismic system. This solution :

- is simple to assemble and install
- adds a minimum mass to the structure
- do not take to much place on the global system

Nevertheless, for the Quad or the BSC-ISI, all the resonances damped have a frequency between 20 Hertz and 1000 Hertz. But the part of the noise, which is important to reduce according to the LIGO system is contained between 0,1 Hertz and 100 Hertz. Thus, this passive solution hasn't had a direct impact on the system, but it is going to be a real profit for the design of the active control loop. The next part of this report will present that.

6. Active damping loop on the BSC-ISI system

Active isolation is used to provide seismic isolation below 20Hz. Both stages are actively controlled. Six electromagnetic actuators, called large actuators, are used between stage 0 and stage 1. Six smaller electromagnetic actuators, called fine actuators, are used between stage 1 and stage 2. The blades, rods and actuators have been positioned to decouple the horizontal and vertical motion of the stages.

6.1 Control Strategy

The feedback control approach is described on the diagram below. Stage 1 is instrumented with 6 Position Sensors (PS), 3 three-axis seismometers (STS) for the low frequency measurements and 6 single axis seismometers (L4C) for the high frequency measurements. Stage 2 is instrumented with 6 Position Sensors (PS), and 6 single axis seismometers (GS13). Although the motions of the stages are coupled to each other, the stages can be controlled independently.

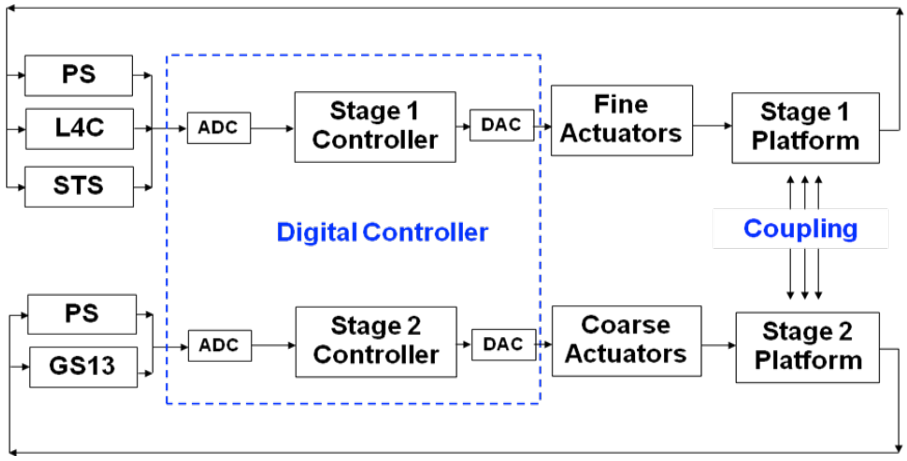

Figure 37 : feedback control approach of the BSC-ISI system

For each stage, the control is based on the use of 6 independent loops. The control is done in the basis of the general coordinate system: X, Y, RZ, Z, RX, RY. X and Y are aligned with the arms of the interferometer. The position sensors are used to measure the relative position of the stage in the direction to be controlled through the Local to General coordinate change of basis matrix (L2G on block 1of the diagram below). The same thing is done with the seismometer to get the inertial motion of the stage in the direction to be controlled in the general basis.

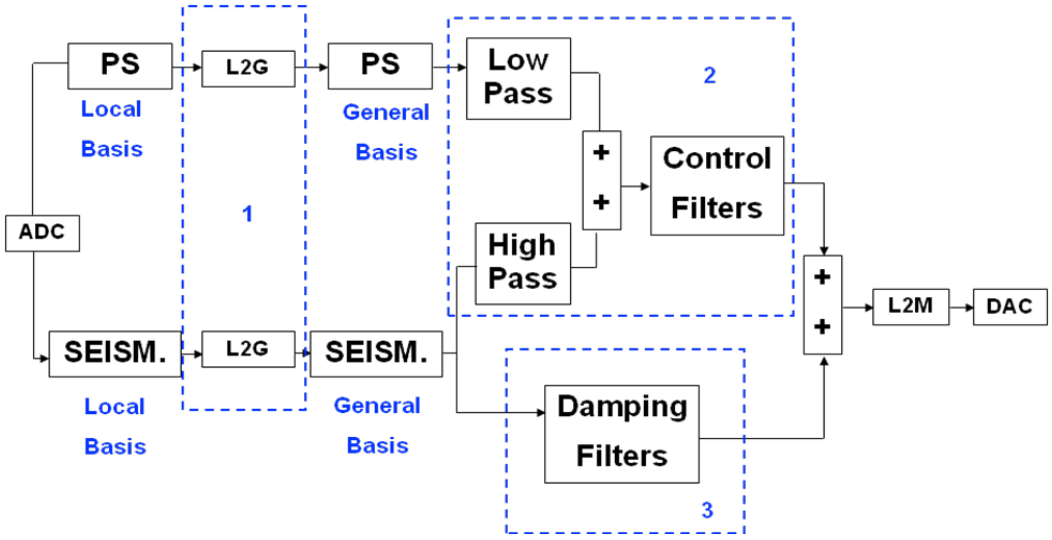

Figure 38 : overview of the control design for the BSC-ISI system

The seismometer signal sensors are first used to damp the suspension resonances (block 3 on the diagram above). Complementary filters are then used to blend the position sensors and the seismometers. The position sensors signal is filtered by the low pass and the seismometer is filtered by the high pass. The two signals are summed resulting in a super sensor (block 2 on the diagram above).

Finally a control filter is applied to the super-sensor to provide loop gain. Those filters typically set the unit gain frequency between 20Hz and 30Hz and the phase margin to 30 degrees.

6.2 Performance

6.2.1 Without a passive solution

The plot below shows the motion of Stage 2 measured in the X direction with the GS13. For this first curve, the active correction has been turned off.

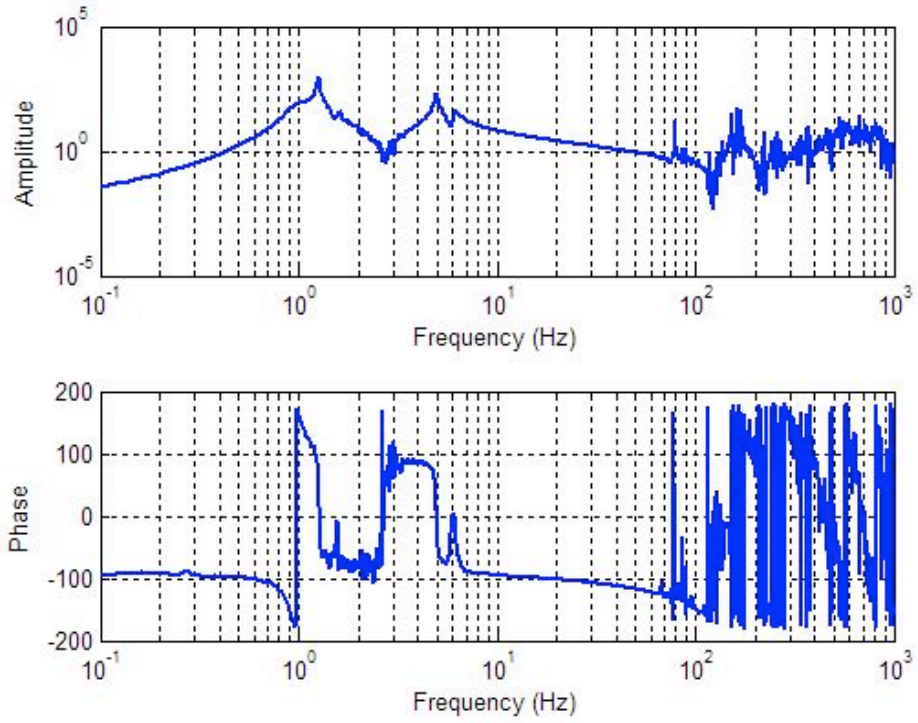

Figure 39 : Transfer function of Stage 2 measured in the horizontal direction

The next step will be to apply an aggressive filter on Stage 2 to improve the performance. This filter must be aggressive, but stable with the time. The objective is to reach a bandwidth from 0,4 Hz to 30 Hz, with almost 30° of phase margin. The next figure presents :

- the plant : the transfer function without the filter
- the controller (Cont) : the behavior of the filter
- the open loop (OL), defines by :

$$OL = Plant*Cont \quad \textbf{(14)}$$

- the close loop (CL) : the transfer function with the filter, defines by :

$$CL = \frac{Plant}{1 + OL} \quad \textbf{(15)}$$

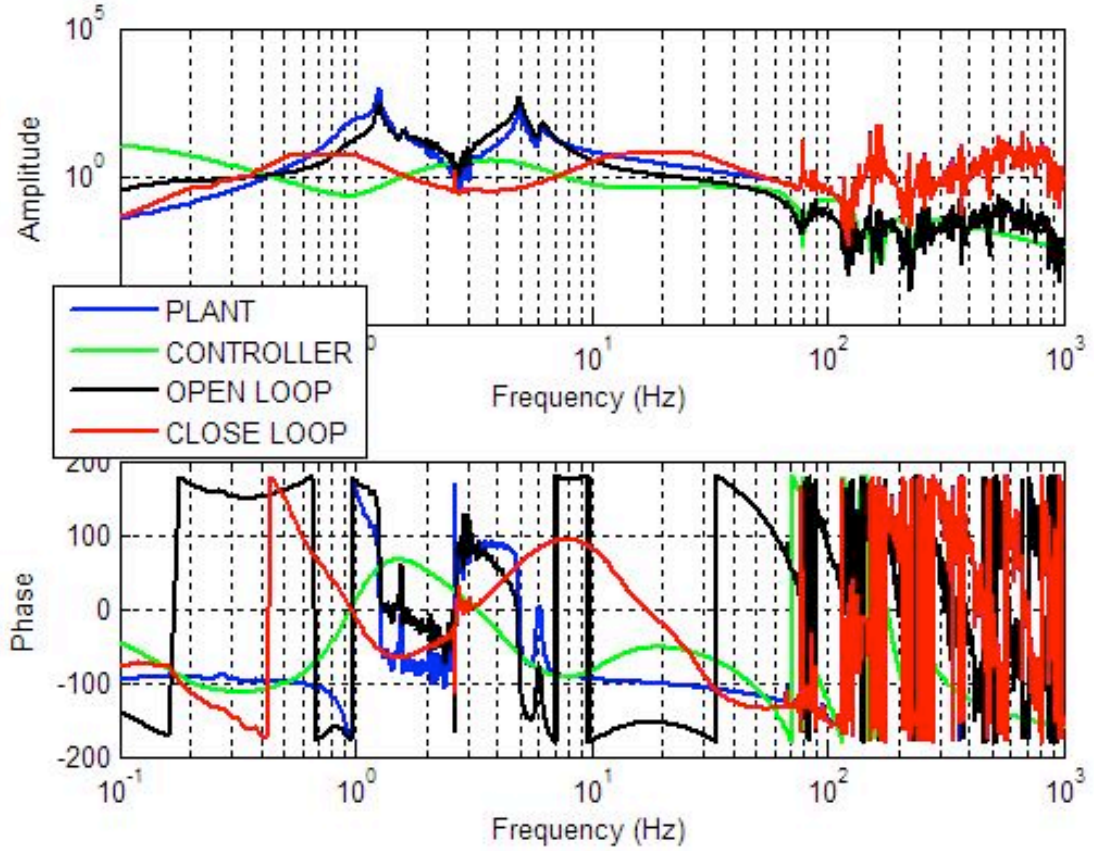

Figure 40 : design of an aggressive filter for Stage 2 transfer function (without mass damper)

The control loop was designed by following some observations :

- At low frequencies (around 0.1Hz) there is very little motion amplification. This is where we usually are at risk to have gain peaking due to the use of a relative displacement signal in the sensors blend. In this case the sensor correction suppresses the gain peaking.

- The isolation starts as low as 0.1Hz which is good. It's usually hard to get isolation at lower frequencies due to the tilt sensitivity of the seismometers.

- The isolation at 1Hz is close to a factor of 100, which means that the position sensor is low passed with an average slope of $1/f^2$, which is good. We could make it slightly more aggressive but it could result in a motion amplification at the blend frequency (0.1Hz).

6.2.2 With a passive solution

The same work is done with the new transfer function of Stage 2, when we add tuned mass dampers.

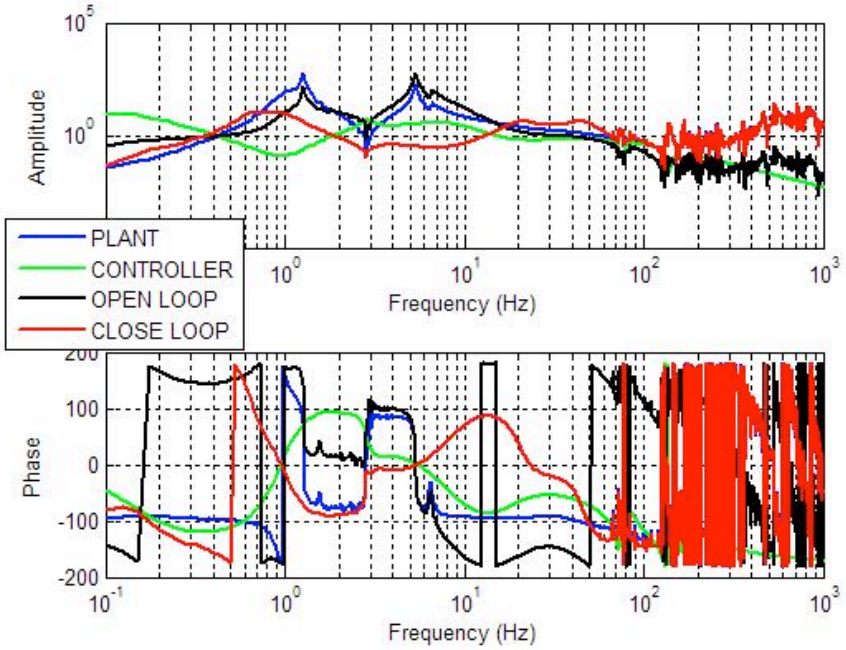

Figure 41 : design of an aggressive filter for Stage 2 transfer function (with mass damper)

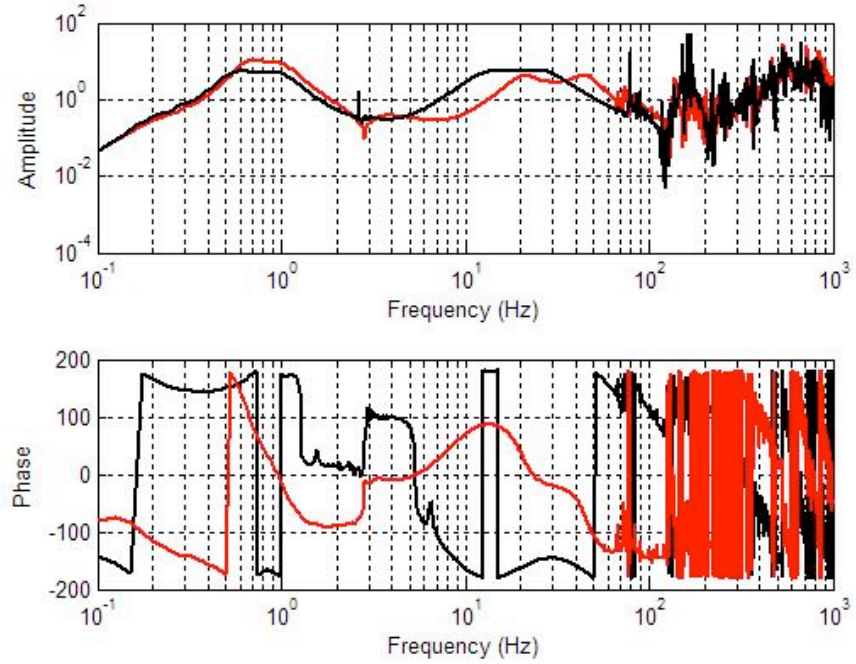

Figure 42 : Comparison of the close loops without mass damper (black curve) and with mass damper (red curve)

The same type of filter is built. But thanks to the passive work done upstream, the performance of the filter can be improve : the damp of the modes between 20 Hz and 1000 Hz allow us to increase the bandwidth and the gain of phase of the filter. Thus we observe an improvement by a factor of 2 between 60 Hertz and 100 Hertz on the new control transfer function, which is a good improvement for the system.

Moreover, less notch filters are used for the new transfer function, which is good. Notch filters are a big source of instability : when frequency change a little with the time (which is the case here), the notch is not going to be effective on the good part of the signal anymore, and will create an instability.

7. Conclusion

During this last six months, several actions have been done to test and design passive damping techniques to improve the performance of seismic isolation system :

- Development of passive damping models with Matlab
- Finite element analysis of mass spring systems using Viton© pads with ANSYS
- Parts and assemblies design for the seismic isolation prototype using Solidworks and PDM Works
- Design and installation of vibration absorbers going from 5 lbs to 200 lbs for structures going from 200 lbs to 600 lbs
- Implementation and testing of damping methods for LIGO suspensions structures
- Modal testing using impact hammers and an accelerometers
- Design and actual implementation of the passive damping approach on the real system
- Design of control loops for the seismic isolation system to evaluate the benefits of the passive damping on the active control (Robustness and Bandwidth improvements)

Some additional activities have also been done (not developed is this report) :

- Design and procurement of mu-metal magnetic shields to minimize the couplings from electromagnetic actuators to seismometers signals

This solution brings a significant improvement for the isolation of the system. The next step is to continue the tests and to develop the device for all the seismic platforms.